

# Two cores in one grain in the microstructure of silicon nitride prepared with aligned whisker seeds

Dong-Soo Park<sup>a,\*</sup>, Tae-Wook Roh<sup>a</sup>, Bernard J. Hockey<sup>b</sup>, Yorinobu Takigawa<sup>c</sup>,  
Byung-Dong Han<sup>a</sup>, Hai-Doo Kim<sup>a</sup>, Yoshiyuki Yasutomi<sup>c</sup>

<sup>a</sup>*Ceramic Materials Group, KIMM, 66 Sang-Nam-Dong, Chang-Won City, Kyong-Nam, South Korea*

<sup>b</sup>*100 Bureau Drive, stop 8521, Gaithersburg, MD 20899-8521, USA*

<sup>c</sup>*R&D Lab., Japan Fine Ceramics Center, 2-4-1 Mutsuno, Atsuta-ku, Nagoya, Japan*

Received 20 September 2001; accepted 7 May 2002

## Abstract

The microstructure of silicon nitride with aligned silicon nitride whisker seeds was examined by electron microscopy. Silicon nitride sintered with yttria and alumina showed a “core-rim” structure. A few grains of the sample sintered with yttria and alumina had more than one core within one grain. This was explained in terms of coalescence of the grains growing from separate cores. A boundary with small misfit was observed by TEM, also supporting the possibility of grain coalescence.

© 2002 Elsevier Science Ltd. All rights reserved.

*Keywords:* Aligned whisker seeds; Coalescence; Core-rim; Silicon nitride

## 1. Introduction

Silicon nitride has been considered as one of the most promising candidates for high temperature structural applications. It shows high strength and fracture toughness among ceramics, and its excellent properties are closely related to the microstructure as evidenced by previous reports.<sup>1–3</sup> Therefore, the microstructure of silicon nitride has been the subject of much research.<sup>4–6</sup> It has been widely accepted that intergranular films of about 1 nm thickness are present between two neighboring grains in silicon nitride.<sup>2,4,7,8</sup> Clarke analyzed the equilibrium thickness of thin intergranular glassy phases based on the van der Waals theory.<sup>9</sup> He obtained the equilibrium thickness of the order of 1 nm for the intergranular glassy phases based on the balance between the attractive force due to long-range van der Waals force and a net repulsive force due to a structural or steric interaction.

One of the recent developments in silicon nitride ceramics is that the microstructural orientation can be controlled by using seed particles of elongated shapes.<sup>10,11</sup>

Silicon nitride with unidirectionally oriented reinforcing grains is reported to exhibit both high strength and fracture toughness at the same time.<sup>10,12</sup> It turns out that silicon nitride with aligned reinforcing grains has not only excellent properties but also interesting microstructural features. Here, some of those microstructural characteristics of silicon nitride prepared with the aligned silicon nitride whisker seeds are reported.

## 2. Experimental

Details of the procedure for sample preparation are described in a previous report.<sup>11</sup> Briefly, tape casting slurry was prepared as follows. For sample A, 88 wt.%  $\alpha$ -Si<sub>3</sub>N<sub>4</sub> powder (E10, Ube Industries, Tokyo, Japan) with 6 wt.% Y<sub>2</sub>O<sub>3</sub> powder (Fine, H.C.Starck, Berlin, Germany) and 1 wt.% Al<sub>2</sub>O<sub>3</sub> powder (AKP30, Sumitomo Chemical Co., Osaka, Japan) were mixed for 4 h using a planetary ball mill. Silicon nitride balls of 5 mm in diameter (SUN11, Nikkato Corp., Tokyo, Japan), a solvent (MIBK, methyl-isobutyl ketone) and a dispersant (Hypermer KD1, ICI Chemical Co., Barcelona, Spain) were used for the first stage of milling. A binder (PVB, polyvinyl butyral, Aldrich Chemical, Milwaukee,

\* Corresponding author.

*E-mail address:* pds1590@kmail.kimm.re.kr (D.-S. Park).

WI, USA) and a plasticizer (dibutyl phthalate, Aldrich Chemical) were added to the jar after the first stage of milling. The milling was resumed for 3.75 h, and then, 5 wt.%  $\beta$ - $\text{Si}_3\text{N}_4$  whiskers (SNWB, Ube Industries) were added to the jar for the final 0.25 h milling. For 120 g of the ceramic ingredients, 160 cc MIBK, 3.6 g Hypermer KD1, 360 g  $\text{Si}_3\text{N}_4$  balls, 38.4 g PVB, and 25.6 cc dibutyl phthalate were used for preparing slip. For sample M, the same procedure as the above was adopted except the starting powder composition. The composition of sample M is 88 wt.%  $\alpha$ - $\text{Si}_3\text{N}_4$ , 6 wt.%  $\text{Y}_2\text{O}_3$ , 1 wt.% MgO (EP, Junsei Chemical Co., Tokyo, Japan), and 5 wt.%  $\beta$ - $\text{Si}_3\text{N}_4$  whisker.

The slurry was poured into the reservoir of the tape casting machine. An array of pins was placed at the exit of the reservoir for facilitating the whisker alignment. The basic idea for employing the array of pins is described in the previous report.<sup>13</sup> The tape was dried over night in open air. After drying, the thickness of the tape was about 120–150  $\mu\text{m}$ . The tape was cut and stacked. Lamination was carried out using a lever press under 30 MPa at 353 K for 0.5 h. Binder removal was performed at 823 K for 10 h. The heating rate was 1.5 K/h. Then, the sample was cold isostatically pressed under 250 MPa after rubber tubing in vacuum.

Gas pressure sintering was carried out at 2123 K for 4 h under 2 MPa nitrogen gas pressure. Samples were fully dense, higher than 99% theoretical. Both the casting surface and the surface normal to the casting direction were machine polished to 1  $\mu\text{m}$  diamond slurry. Plasma etching was performed with equal volume percents of  $\text{CF}_4$  and  $\text{O}_2$  gas. The microstructure was examined using SEM after gold coating. Length and width of the grains were measured using an image analysis software (Image-Pro 3.0, Media Cybernetics, L.P., Silver Spring, MD, USA). The plasma-etched sample was carbon coated for field emission gun SEM (FEG-SEM, JSM6330F, Jeol Ltd., Tokyo, Japan) observation. The specimen was tilted 70° to provide a stereoscopic image. TEM samples were prepared according to the standard TEM sample preparation procedure after slicing the sintered samples either normal to the casting direction or parallel to the casting surface.

### 3. Results and discussion

Fig. 1(a) shows a SEM micrograph of the casting surface of sample A after sintering. The large grains of sample A are highly aligned and they have a core-rim structure. The core is supposed to be the  $\beta$ - $\text{Si}_3\text{N}_4$  whisker of high purity while the rim is  $\beta$ -sialon as shown in EDS spectra of Fig. 1(b).<sup>14</sup> It has been reported that  $\beta$ - $\text{Si}_3\text{N}_4$  with no  $\text{Al}_2\text{O}_3$  is more deeply etched than the sialon solid solution.<sup>5</sup> Closer examination of the core-rim structure reveals that the grain growth occurs much faster in the length direction than in the width direction.

Lengths and widths of 31 grain-core pairs in Fig. 1 were measured using the image analysis software. Ratios of length and width the grains and the corresponding cores were  $4.16 \pm 1.28$  and  $2.72 \pm 1.45$ , respectively. This confirms that the grain growth occurs preferentially in the length direction, as schematically expressed in Fig. 2. Meanwhile, average length and width of the longest 550 elongated grains in Fig. 1(a) were 23.9 and 3.6  $\mu\text{m}$ , respectively.

Fig. 3(a) shows that there are two cores in one grain of sample A. Grain growth of silicon nitride occurs by a solution-precipitation process. In other words, grains smaller than the critical size disappear and larger ones grow. When two grains larger than the critical size come into contact, there is a glassy grain boundary between those two grains as reported by many previous workers.<sup>7–9</sup> Therefore, each grain has one core on which the grain grows. One possible explanation for the two cores in one grain shown in Fig. 3(a) is grain coalescence. According to German,<sup>15</sup> grain coalescence is easiest when the two grains in contact have similar orientation, but this is a low probability situation. When the grains are randomly oriented, grain coalescence is a rare occurrence. However, the probability of grain coalescence is certainly increased by aligning those elongated grains. Fig. 1 shows how well aligned are the large elongated grains of sample A. Alignment of those elongated grains results from that of the whisker seeds. During sintering, grain growth occurs on those whisker seeds. Two neighboring grains growing from two whiskers of similar orientations come into contact, and, then, the grain boundary is replaced by a sub-boundary.

Fig. 3(b) is an FEG-SEM micrograph of sample A that shows a stereoscopic image of the sample. It clearly shows that the grains were etched deeper than the grain boundary and core was etched even deeper than the grain. Even though the glassy grain boundary was as thin as 1 nm, its presence is well recognized from the micrograph. A grain with two cores that is similar to the one shown in Fig. 3(a) is shown in Fig. 3(b). Also, it is noticed that there is no glassy intergranular boundary between the two grains as indicated by the arrow in Fig. 3(b). The disappearance of glassy intergranular boundary between the two grains is explained by grain coalescence as described above. Only a few grains appear to have a core in Fig. 3(a) and (b). That is not because most grains do not have a core, but because the probability of cutting the core for observation is low, less than 25%. Fig. 4(a) shows a TEM micrograph of the sample cut normal to the casting direction and Fig. 4(b) shows SAD pattern from the three grains marked as A, H and I in Fig. 4(a). SAD pattern of the three grains reveals that misorientation of the three grains from [0001] direction was within 2 degrees. Therefore, misorientation among the grains was small enough to replace intergranular glassy phase with low angle boundary and to allow grain coalescence. Also,

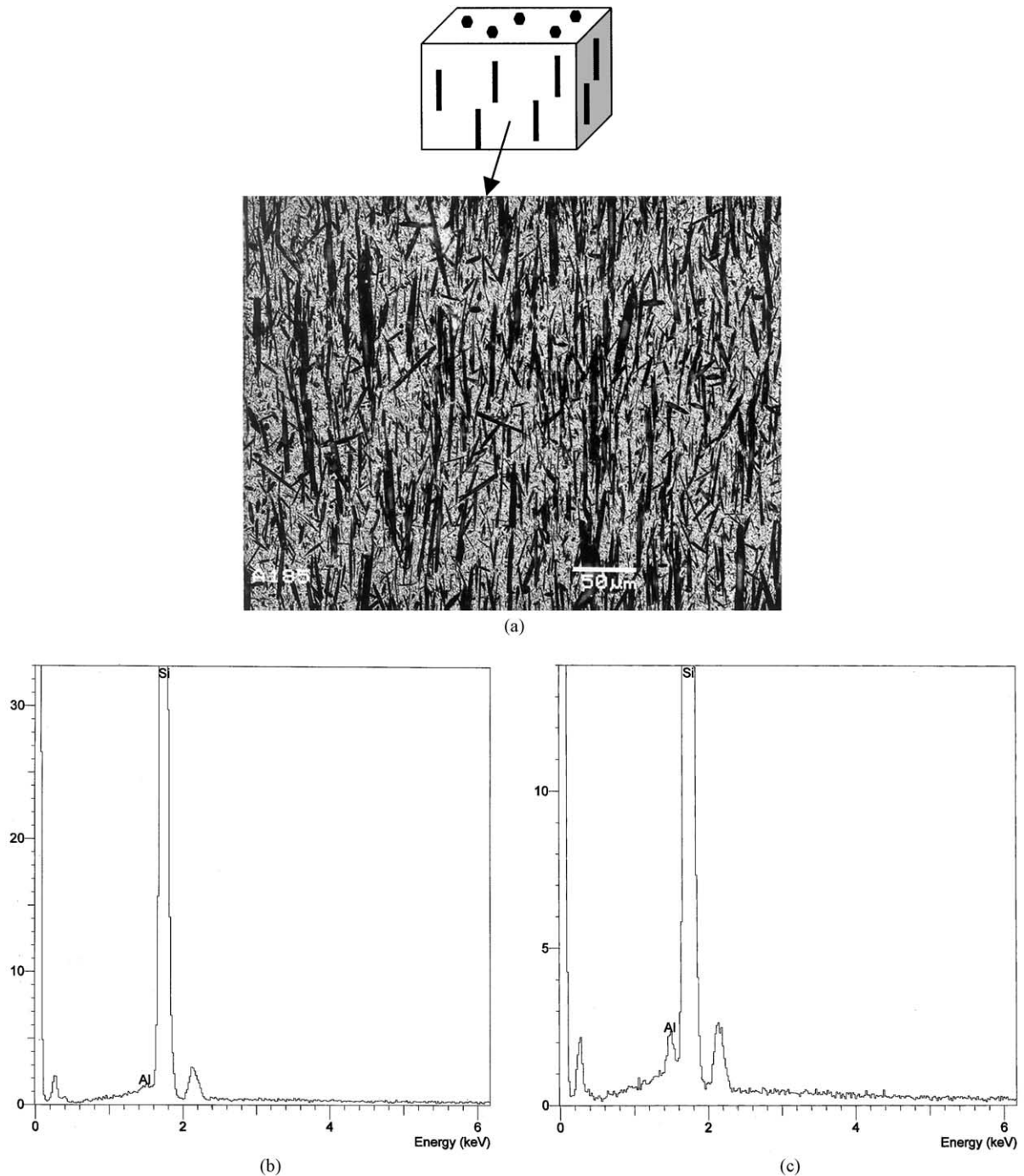


Fig. 1. SEM micrograph and EDS of the casting surface of sample A after plasma-etching; (a) SEM micrograph, (b) EDS spectrum from core and (c) EDS spectrum from rim.

crystalline phase at the triple point was observed as was reported by Vetrano et al.<sup>16</sup>

In the case of sample M, there is no distinction between the core and the rim as shown in Fig. 5. This is due to the fact that none of the sintering additives,  $Y_2O_3$  and MgO, is involved in forming the rim around the silicon nitride whisker core. In other words, unlike sample A, the chemical composition of the rim of sample M is similar to that of the core, and there is no difference

between the plasma-etching rates of the core and the rim. The sample was tilted at  $45^\circ$  to provide a stereoscopic image of the microstructure that showed the grain boundary more clearly. It is clearly recognized that the glassy grain boundary appearing as bright linear network disappeared at the regions marked by arrows between the grains. It is understood in Fig. 5 that two grains with similar orientations in sample M were also coalesced into one grain.

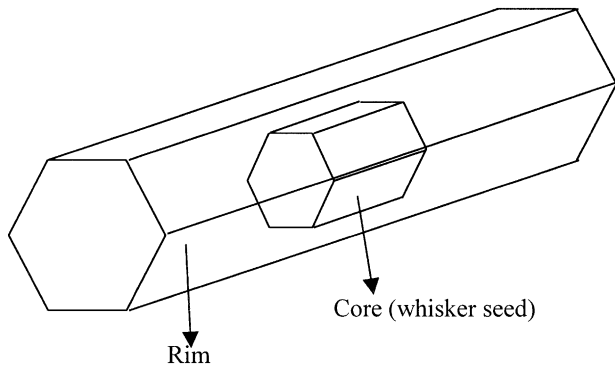


Fig. 2. A schematic diagram of grain growing from the whisker seed.

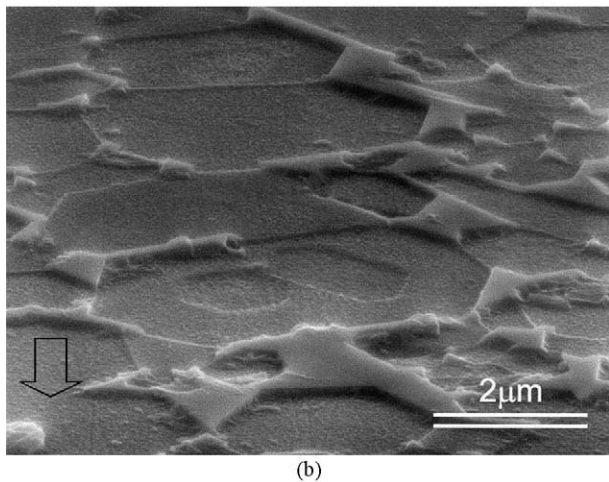
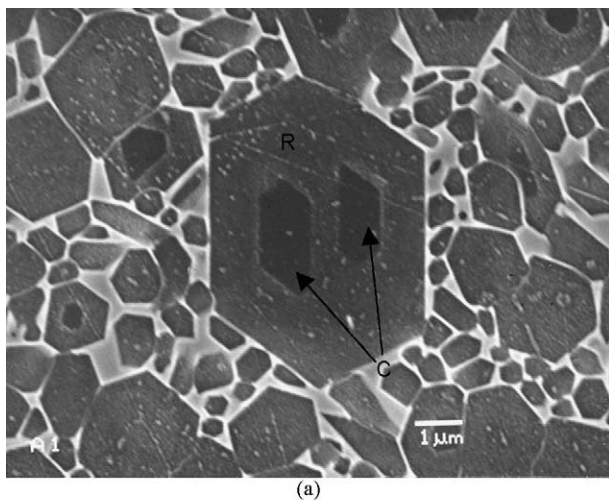
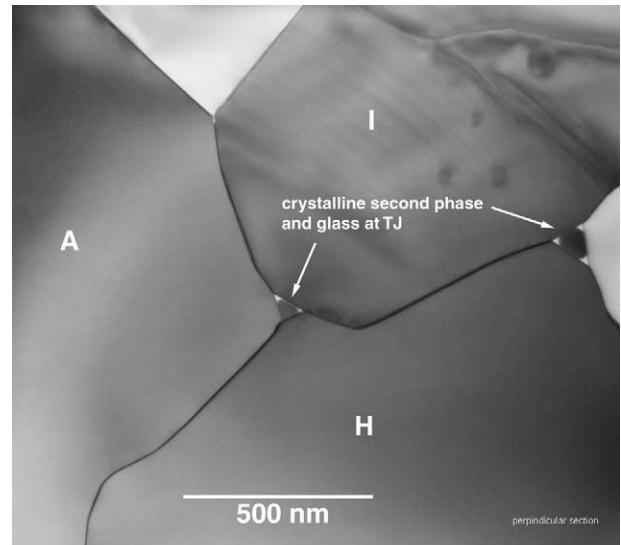
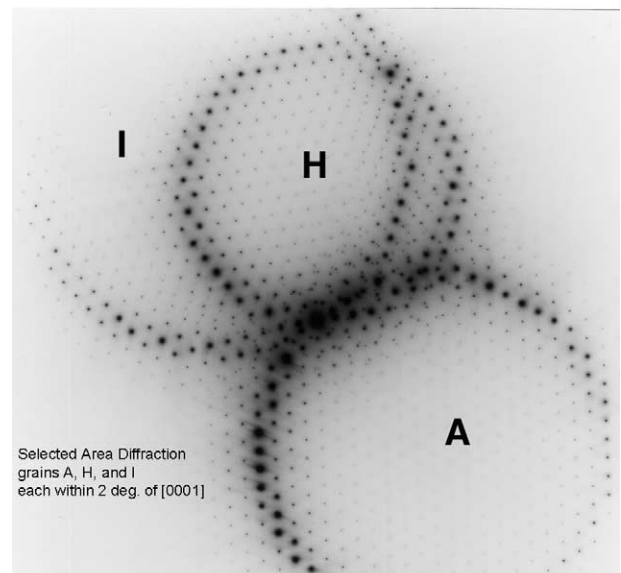


Fig. 3. SEM micrographs of samples after plasma etching; (a) sample A showing a grain with two cores: “C” represents the core and “R” the rim, (b) FEG-SEM micrograph of sample A.

Fig. 6(a) and (b) show SEM micrographs of the casting surface of sample A. Fig. 6(a) shows that the large elongated grain has two cores. Higher magnification micrograph of the area between the two arrows in Fig. 6(a) is shown in Fig. 6(b). Fig. 6(b) shows that the



(a)



(b)

Fig. 4. TEM micrograph (a) and SAD pattern (b) of sample A; TEM sample was cut normal to the casting direction.

area between the two cores contains pores. When the two grains approach each other close enough, atomic bonding across the grain boundary forms simultaneously at many locations as reported for the sapphire crystals.<sup>17</sup> The grain boundary liquid phase is squeezed out of the bonded area that grows rapidly. Since the bonded area grows quickly and simultaneously at many locations, some liquid is possibly trapped. It is not clear at this point how the entrapped liquid disappears leaving a pore. Fig. 7 shows TEM micrograph of sample A that was cut parallel to the casting direction. A large elongated grain in Fig. 7 contains a dislocation network. It is suspected that the dislocation network shown in Fig. 7 is formed to compensate the mismatch between the two grains during the coalescence.

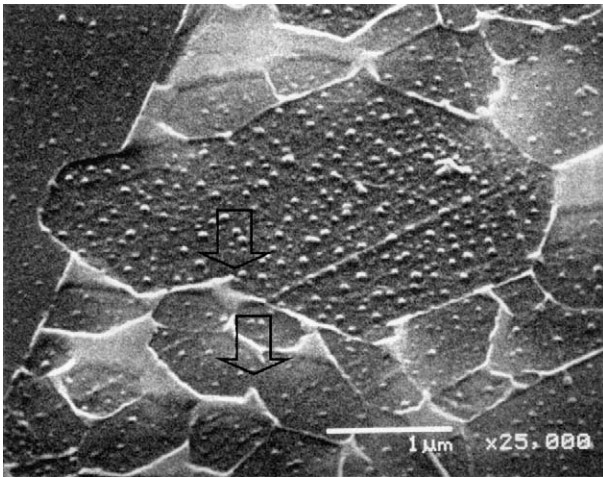
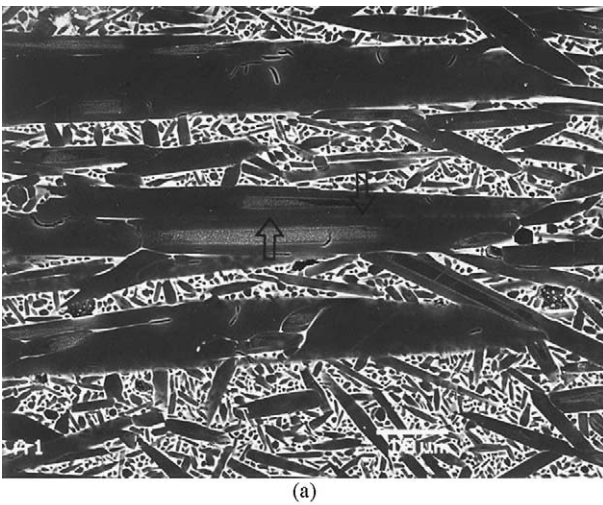
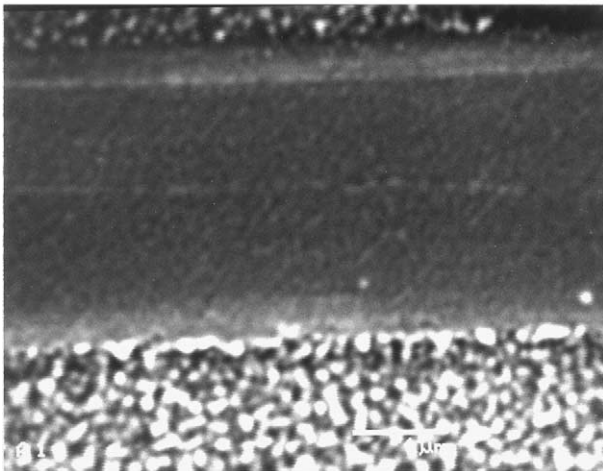


Fig. 5. SEM micrograph of sample M after plasma etching; the sample was tilted at 45° for better observation of the grain boundary.



(a)



(b)

Fig. 6. SEM micrographs of grain with two cores on the casting surface of sample A; (a) lower magnification and (b) higher magnification of the area between the two arrows in (a).

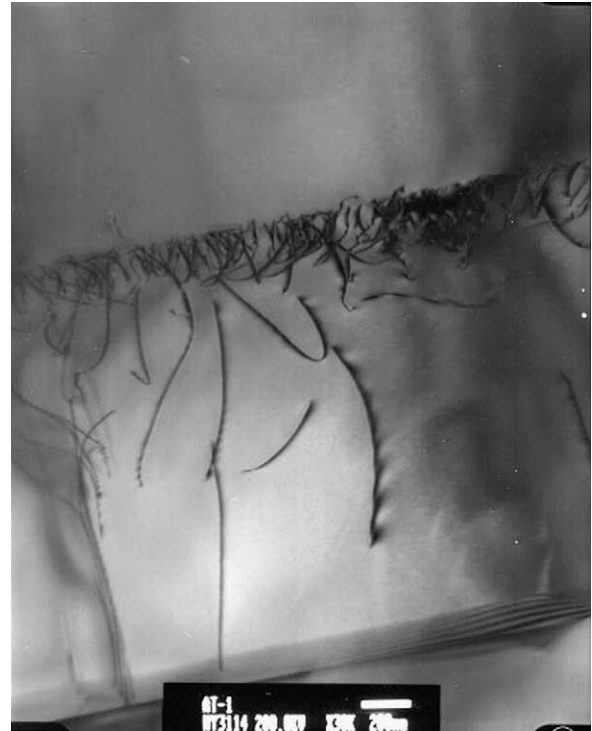


Fig. 7. TEM micrograph of sample A; TEM sample cut parallel to the casting surface.

#### 4. Conclusion

Silicon nitride with highly aligned silicon nitride whisker seeds showed a unique microstructure. Some of the grains have more than one core. Morphology of those grains indicates that coalescence of grains growing from separate cores occurred. TEM analyses reveal that misorientation between the grains was small enough to replace the glassy grain boundary with low angle boundary.

#### Acknowledgements

This work was supported by the NRL program of the Korean Ministry of Science and Technology. We acknowledge Professor Doh-Yeon Kim at Seoul Nat'l Univ., Seoul, South Korea for helpful discussions.

#### References

1. Ziegler, G., Heinrich, J. and Woetting, G., *Review: relationships between processing, microstructure and properties of dense and reaction-bonded silicon nitride*. *J. Mater. Sci.*, 1994, **22**, 3041–3086.
2. Park, H., Kim, H.-E. and Niihara, K., *Microstructural evolution and mechanical properties of Si<sub>3</sub>N<sub>4</sub> with Yb<sub>2</sub>O<sub>3</sub> as a sintering aid*. *J. Mater. Res.*, 1999, **14**(5), 1904–1909.
3. Pyzik, A. J. and Beaman, D. R., *Microstructure and properties of self-reinforced silicon nitride*. *J. Am. Ceram. Soc.*, 1993, **76**(11), 2737–2744.

4. Lange, F. F., Silicon nitride polyphase systems: fabrication, microstructure and properties. *Int. Metals Rev.*, 1980, **1**(1), 1–20.
5. Hoffmann, M. J., Analysis of microstructural development and mechanical properties of  $\text{Si}_3\text{N}_4$  ceramics. In *Nato ASI Series E: Applied Sciences Vol. 276, Tailoring of Mechanical Properties of  $\text{Si}_3\text{N}_4$  Ceramics*, ed. M. J. Hoffmann and G. Petzow. Kluwer Academic Press, Netherlands, 1994, pp. 59–72.
6. Hirosaki, N., Tanimura, M., Okamoto, Y., Akimune, Y. and Mitomo, M., TEM analysis of core/rim structure in  $\beta$ -silicon nitride ceramics. *J. Ceram. Soc. Jpn.*, 1994, **102**(9), 875–879.
7. Clarke, D. R., On the equilibrium thickness of intergranular glass phases in ceramic materials. *J. Am. Ceram. Soc.*, 1987, **70**(1), 15–22.
8. Kleebe, H.-J., Structure and chemistry of interfaces in  $\text{Si}_3\text{N}_4$  ceramics studied by transmission electron microscopy. *J. Ceram. Soc. Jpn.*, 1997, **105**(6), 453–475.
9. Clarke, D. R. and Thomas, G., Grain boundary phases in a hot-pressed MgO fluxed silicon nitride. *J. Am. Ceram. Soc.*, 1977, **60**(11–12), 491–495.
10. Hirao, K., Ohashi, M., Brito, M. E. and Kanzaki, S., Processing strategy for producing highly anisotropic silicon nitride. *J. Am. Ceram. Soc.*, 1995, **78**(6), 1687–1690.
11. Park, D.-S. and Kim, C.-W., Indentation crack length anisotropy in silicon nitride with aligned reinforcing grains. *J. Am. Ceram. Soc.*, 2000, **83**(3), 663–665.
12. Becher, P. F., Sun, E. Y., Plucknett, K. P., Alexander, K. B., Hsueh, C.-H., Lin, H.-T., Waters, S. B., Westmoreland, C. G., Kang, E.-S., Hirao, K. and Britio, M. E., Microstructural design of silicon nitride with improved fracture toughness: I, effects of grain shape and size. *J. Am. Ceram. Soc.*, 1998, **81**(11), 2821–2830.
13. Park, D.-S., Kim, C.-W., Park, C. and Yoo, B.-J., Silicon nitride containing unidirectionally oriented silicon nitride whiskers prepared by tape casting. In *Ceramic Transactions, Ceramic Matrial Systems with Composite Structures*, ed. N. Takeda, L. M. Sheppard and J.-I. Kon. American Ceramic Society, Westerville, OH, 1998, pp. 3–15.
14. Park, D.-S. and Kim, C.-W., Anistropy of silicon nitride with aligned silicon nitride whiskers. *J. Am. Ceram. Soc.*, 1999, **82**, 780–782.
15. German, R. M., *Liquid Phase Sintering*. Plenum Press, NY, 1985.
16. Vetrano, J. S., Kleebe, H.-J., Hampp, E., Hoffmann, M. J. and Cannon, R. M., Epitaxial deposition of silicon nitride during post-sintering heat treatment. *J. Mater. Sci.*, 1992, **11**, 1249–1252.
17. Kim, D.-Y., Wiederhorn, S. M., Hockery, B. J., Handworker, C. A. and Blendell, J. E., *J. Am. Ceram. Soc.*, 1994, **77**, 444–453.